# Effects of Alloying Elements on Cold Crack Susceptibility in 0.1%C Basic Steels with Implant Test †

Fukuhisa MATSUDA*, Hiroji NAKAGAWA** and Shunichi KATOH***

**Abstract**

*In this report the implant cracking test was applied as a cold cracking test for basic 0.1% carbon steels alloyed with nickel, chromium, molybdenum or manganese. The microstructures and maximum hardness in Vickers hardness test in the heat-affected zone were investigated. The delayed crack occurred in the 0.1%C basic steels which contained alloying element more than about 5% in Ni, 4% in Cr, 1% in Mo or 2% in Mn.*

*The maximum hardness in the heat-affected zone at which the delayed crack occurred was more than about 300 to 350. The microstructure of the heat-affected zone of the steels in which the delayed crack occurred mainly showed a bainitic and martensitic structure without primary ferrite along the prior-austenite boundary.*

**KEY WORDS:** (Implant Tests) (Microstructure) (Ferrite) (Grain Boundaries) (Heat Affected Zone) (Hardness) (Cold Cracking)

## 1. Introduction

Cold crack in low alloy high strength steel is one of the most serious problems encountered during welding performance. It is generally known that cold cracks in low carbon-low alloy steels are mainly caused by hydrogen embrittlement. Therefore, there are many reports which deal with hydrogen embrittlement in relation to alloy elements, microstructure, weld heat input, diffusible hydrogen content, restraint stress and so on. Recently the implant cracking test has been widely used to investigate the cold crack susceptibility in heat-affected zone (HAZ), since it enables in various hydrogen levels to easily study the relationship between applied stress and fracture time. In this report the implant cracking test was applied as a cold cracking test for basic 0.1% carbon steels alloyed with nickel, chromium, molybdenum or manganese.

## 2. Experimental Procedure

A special characteristic of the implant test is that a small sample is utilized to inverstigate the crack susceptibility. The specimen in the implant cracking test used was 6 millimeters in diameter, and was machined with the axis parallel to the direction of the hot working process. Then, a spiral notch was machined in order to avoid scattering of the data which might be caused by a penetration error in fusion boundary, the details of which are illustrated in **Fig. 1**. The load is applied by a constant dead weight with a lever. The chemical compositions of steels used in this experiment are listed in **Table 1**. Ni, Cr, Mo and Mn were respectively added in about 0.1%C basic steels.

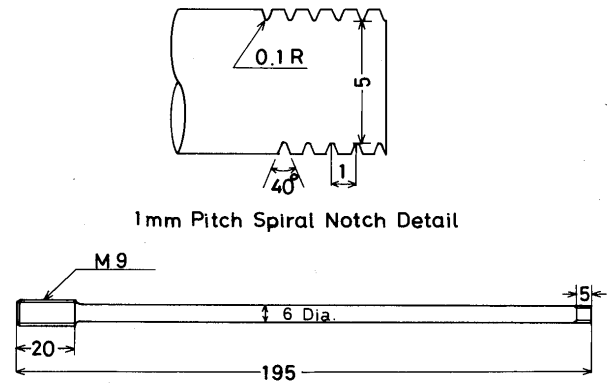


**Fig. 1** Implant specimen details

As the backing plate, JIS SM50 of 20 mm in thickness, 200 mm in width and 300 mm in length was used. A bead-on-plate welding of 100 mm in length on the backing plate was completed using a welding condition of arc voltage of 25 volts, a welding current of 170 amperes and welding speed of 150 mm/min; that is to say, 17kJ/cm of weld heat input. The specification of manual covered electrode used is shown in **Table 2**. The cooling time from 800°C to 500°C in the fusion boundary was about 6 seconds.

† Received on April 4, 1980
* Professor
** Reseach Instructor
*** Associate Professor, Hachinohe Technical College

Transactions of JWRI is published by Welding Research Institute of Osaka University, Suita, Osaka, Japan

Table 1 Chemical composition of steels used

| Steel | Chemical Composition (%) | | | | | | Vickers hardness of base metal (Hv) | Tensile strength ($kg/mm^2$) |
|---|---|---|---|---|---|---|---|---|
| | C | Si | Mn | Ni | Cr | Mo | | |
| Ni-1 | 0.08 | – | – | – | – | – | 87 | 28.1 |
| Ni-2 | 0.15 | – | – | 2.43 | – | – | 118 | 37.3 |
| Ni-3 | 0.12 | – | – | 3.49 | – | – | 126 | 39.3 |
| Ni-4 | 0.16 | – | – | 5.06 | – | – | 141 | 44.6 |
| Ni-5 | 0.13 | – | – | 7.02 | – | – | 153 | 49.9 |
| Ni-6 | 0.10 | – | – | 9.11 | – | – | 177 | 54.3 |
| Cr-1 | 0.11 | 0.22 | 0.46 | – | – | – | 105 | 28.5 |
| Cr-2 | 0.11 | 0.22 | 0.36 | – | 0.47 | – | 101 | 38.0 |
| Cr-3 | 0.10 | 0.23 | 0.35 | – | 1.00 | – | 127 | 39.5 |
| Cr-4 | 0.10 | 0.23 | 0.35 | – | 1.97 | – | 133 | 44.0 |
| Cr-5 | 0.09 | 0.22 | 0.37 | – | 3.86 | – | 242 | 71.2 |
| Mo-1 | 0.11 | 0.22 | 0.46 | – | – | – | 105 | 28.5 |
| Mo-2 | 0.12 | 0.16 | 0.45 | – | – | 0.48 | 122 | 41.3 |
| Mo-3 | 0.11 | 0.23 | 0.43 | – | – | 0.96 | 166 | 48.6 |
| Mo-4 | 0.11 | 0.22 | 0.37 | – | – | 1.06 | 176 | 59.0 |
| Mn-1 | 0.11 | 0.21 | – | – | – | – | 105 | 39.1 |
| Mn-2 | 0.11 | 0.22 | 0.46 | – | – | – | 105 | 28.5 |
| Mn-3 | 0.11 | 0.21 | 1.06 | – | – | – | 136 | 43.8 |
| Mn-4 | 0.12 | 0.21 | 2.05 | – | – | – | 167 | 56.1 |

Table 2 Specification of covered electrode used

| Grade in JIS | Type of coating | Diameter | Diffusible hydrogen content in JIS method | Condition for drying |
|---|---|---|---|---|
| D4301 | ilumenite | 4 mm | 34.1 cc | 120°C x 1 hr |

Then a load was applied to the specimen at one minute after the test welding was completed. The temperature around the spiral notch of the specimen at that time was 120 to 150°C. The maximum testing time was limited to 24 hours. The maximum value of the stress which did not cause the fracture after the lapse of 24 hours was determined and this lower critical stress was taken as the parameter of the crack susceptibility. The microstructures and maximum hardness in Vickers hardness (Hv) test in the heat affected zone were investigated.

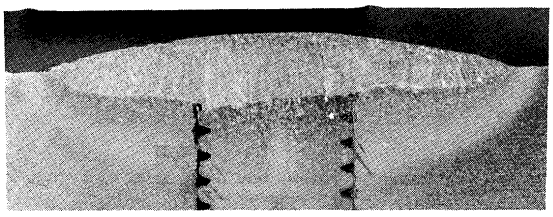

Photo 1. Heat affected zone of implant, (Cr-5), x 3.3

## 3. Experimental Result

A typical example of penetration in crosssection is shown in **Photo 1.**

### 3.1 Ni-alloyed steel

**Figure 2** shows change in the hardness of the base metal and the maximum hardness (Hv max) in the heat-affected zone caused by varying nickel content. As the nickel content increases the maximum hardness in the heat-affected zone shows its maximum value at about 5 percent nickel content level. **Figure 3** shows the relation between applied stress and fracture time, in which delayed crack didn't occur in Ni-1, Ni-2 and Ni-3. The lower critical stresses are respectively determined as 42, 40 and 30 $kg/mm^2$ in Ni-4, Ni-5 and Ni-6. Thus, the delayed cracking occurred at more than Hv350. As the nickel con-

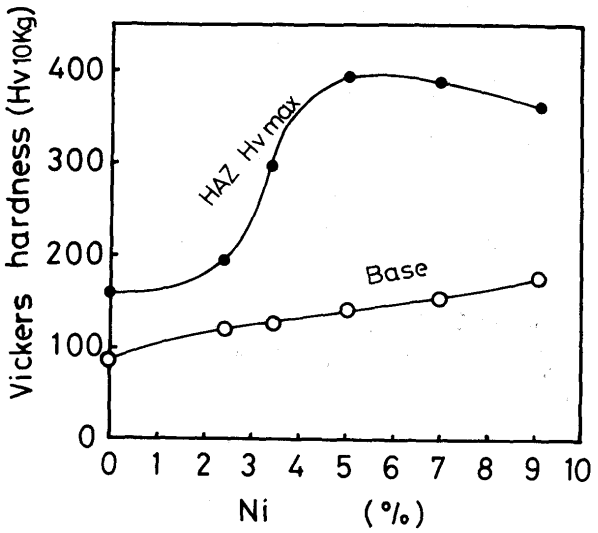


Fig. 2 Effect of Ni on the hardness in base metal and HAZ

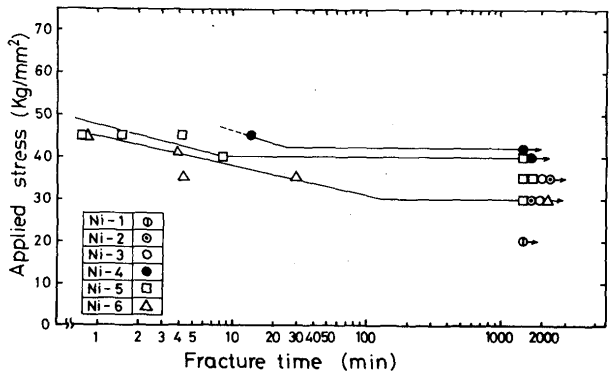


Fig. 3 Relation between applied stress and fracture time in Ni-alloyed steel

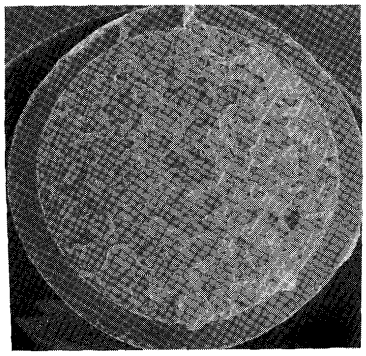

Photo 2. Example of macrofractograph, Ni-4, $\sigma$=45 kg/mm$^2$, fracture time: 13.8min, x 7

Photo. 3 Example of microfractograph, Ni-4, $\sigma$=45 kg/mm$^2$, fracture time: 13.8 min, x 1500

tent increases, the tensile strength increases as shown in Table 1, but the value of the lower critical stress decreases as shown in Fig. 3. **Photograph 2** shows an example of the macrofractographs of Ni-4 steel. **Photograph 3** shows quasicleavage fractures observed by scanning electron microscope (SEM) in the Ni-4 fractured implant specimen with an applied stress of 45 kg/mm$^2$. **Photograph 4** shows the microstructures of the heat affected zones near the fractured surface in nickel-alloyed steel.

With increasing in nickel content, the coarse ferrite formed along the prior-austenite grain boundary was reduced in the amount, and from Ni-4 (about 5% Ni) the ferrite was scarecely observed at the grain boundaries. This well agrees with the transformation limit of the proeutectoid ferrite designated in $C_f$, in CCT diagram which was reported by Inagaki et al[1]. That is to say, $C_f$' in 5% Ni steel is about 6 seconds, which is equal to the cooling time from 800 to 500°C in this study.

### 3.2 Cr-alloyed steel

**Figure 4** shows the hardness of the base metal and the maximum hardness in the heat-affected zone. Both the base metal and the heat-affected zone show a tendency to increase monotonously with chromium content. **Figure 5** shows the relation between applied stress and fracture time in which delayed crack didn't occur in Cr-1, 2, 3 and 4. A lower critical stress was obtained in the case of the Cr-5 alloy steel as about 50 kg/mm$^2$. As the applied stress approaches the tensile strength a considerable scattering can be seen. According to the maximum hardness curve in the heat affected zone in Fig. 4, the delayed cracking occurred at 350 in hardness. **Photographs 5** and **6** show macro and micro fractographs with intergranular and quasi-cleavage fracture surface of Cr-5 specimen fractured in an applied stress of 60 kg/mm$^2$ observed by SEM. **Photograph 7(a)**, **(b)** and **(c)** show the microstructure of the heat-affected zones of Cr-3, Cr-4 and Cr-5 steels respectively. In the heat-affected zone of Cr-3 and Cr-4 steels, obvious ferrite was observed along the prior-austenite grain boundary, but in Cr-5 there was no ferrite

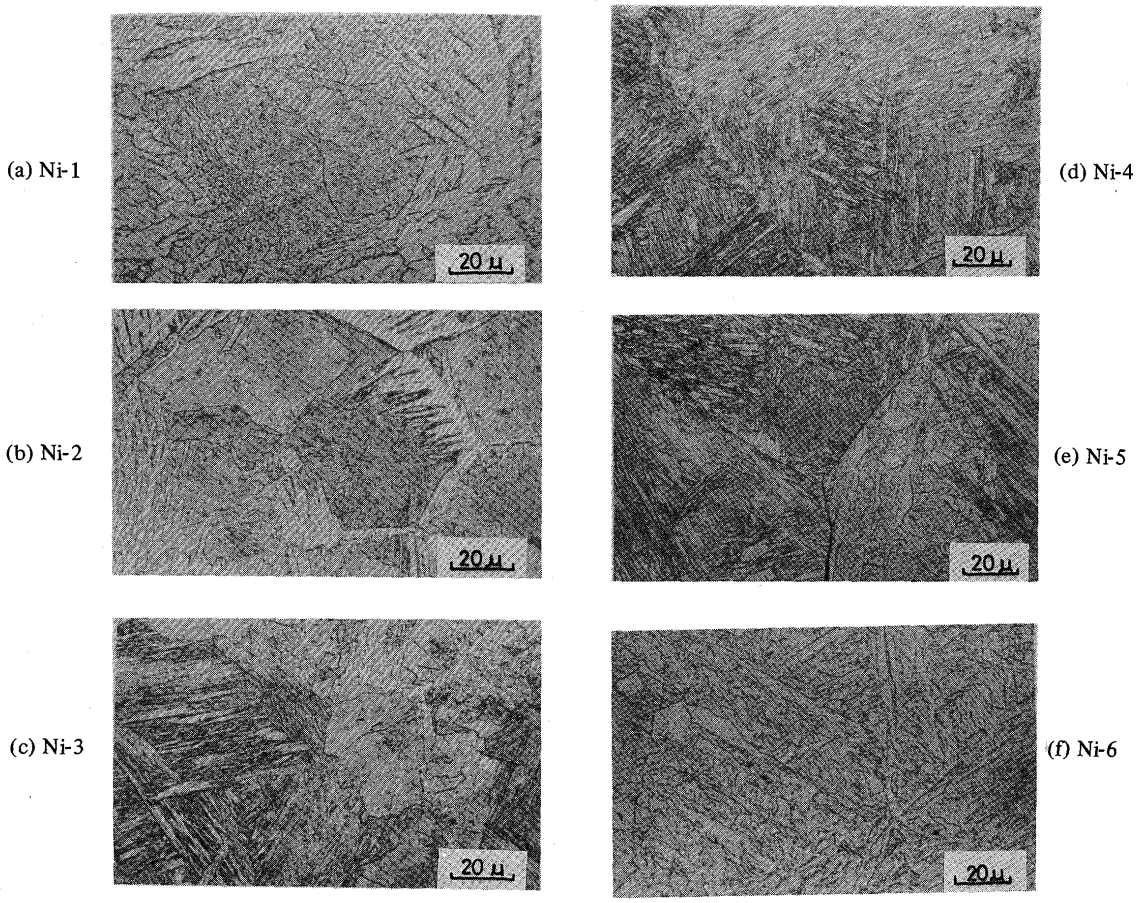


**Photo 4.** Effect of Ni on microstructure in HAZ

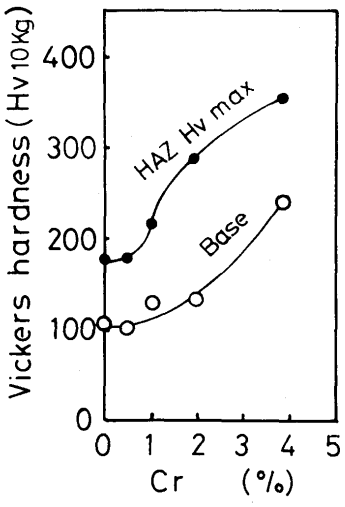


**Fig. 4** Effect of Cr on the hardness in base metal and HAZ

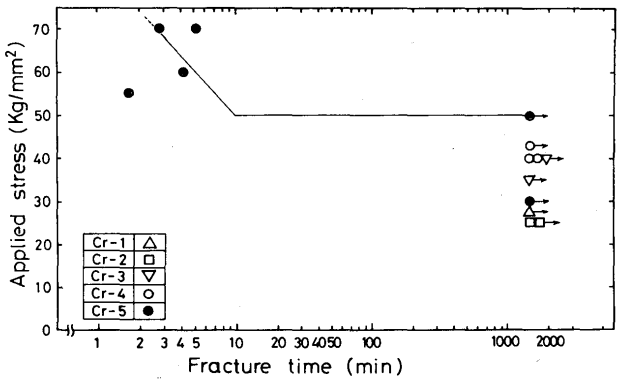


**Fig. 5** Relation between applied stress and fracture time in Cr-alloyed steel

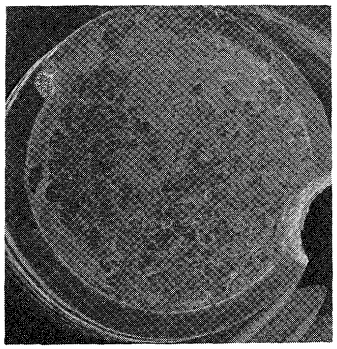

**Photo. 5** Example of microfractograph, Cr-5, $\sigma$=60 kg/mm$^2$, fracture time: 4.2 min, × 7

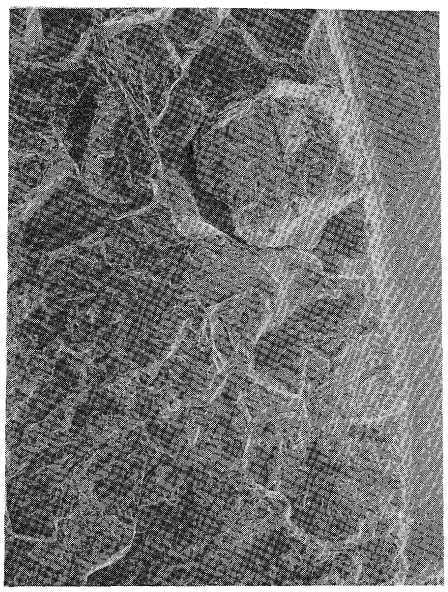

Photo 6. Example of microfractograph Cr-5, $\sigma$=60 kg/mm$^2$, fracture time: 4.2 min, x 60

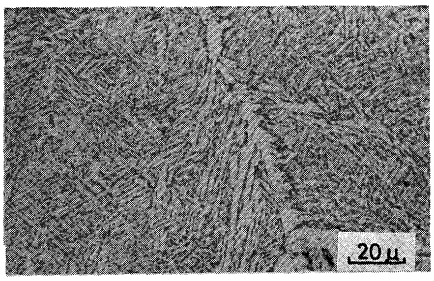


(a) Cr-3

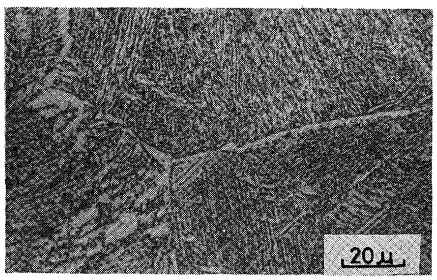


(b) Cr-4

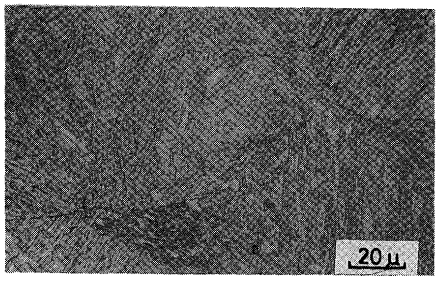


(C) Cr-5

Photo 7. Effect of Cr on microstructure in HAZ

except bainite and martensite structures. This also well agrees with the result in CCT diagram by Inagaki et al[2].

### 3.3 Mo-alloyed steel

**Figure 6** shows the hardness of the base metal and the maximum hardness in the heat-affected zone caused by varying molybdenum content. The maximum hardness in the heat-affected zone shows a tendency to increase with molybdenum content. The delayed cracking occurred only in the Mo-4 alloy whose maximum hardness showed about 300. **Figure 7** shows the relation between molybdenum-alloyed steels and fracture time. **Photographs 8** and **9** show the macro and micro fractographs of

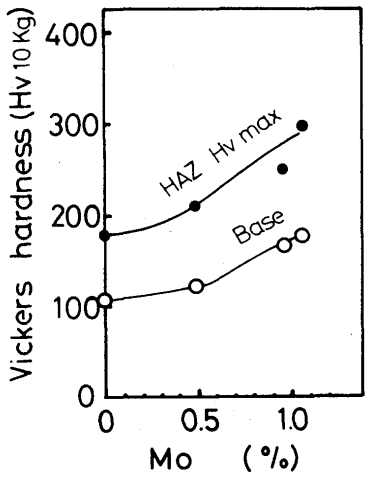


Fig. 6 Effect of Mo on the hardness in base metal and HAZ

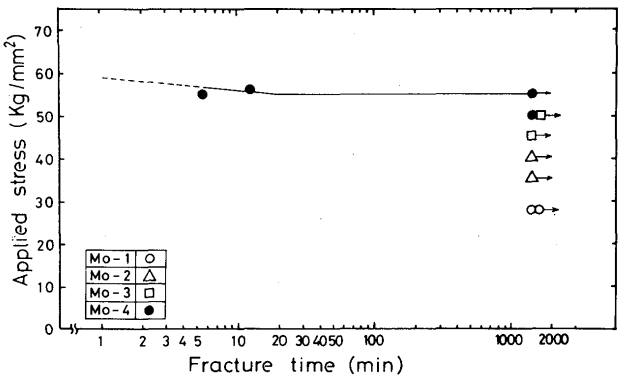


Fig. 7 Relation between applied stress and fracture time in Mo-alloyed steel

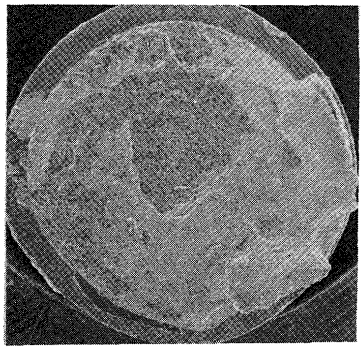

Photo 8. Example of macrofractograph, Mo-4, $\sigma$=55 kg/mm$^2$, fracture time: 5.7 min, x 7

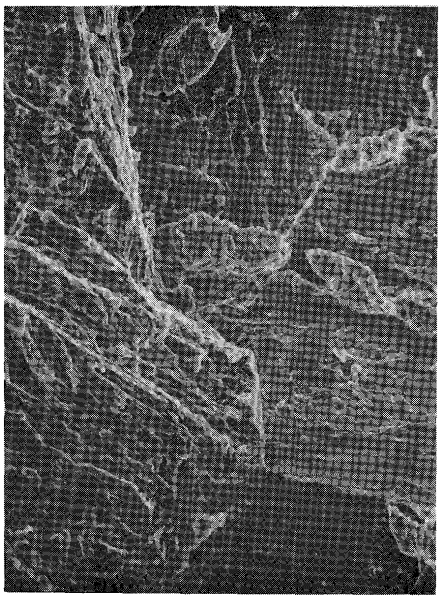

Photo 9. Example of microfractograph, M0-4, $\sigma$=55 kg/mm, fracture time: 5.7 min, x 600

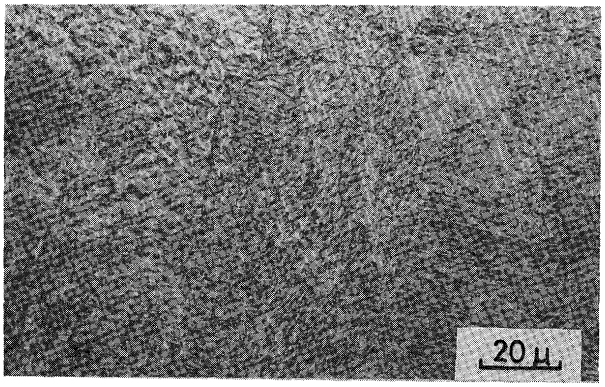


Photo 10. Effect of Mo on microstructure in HAZ

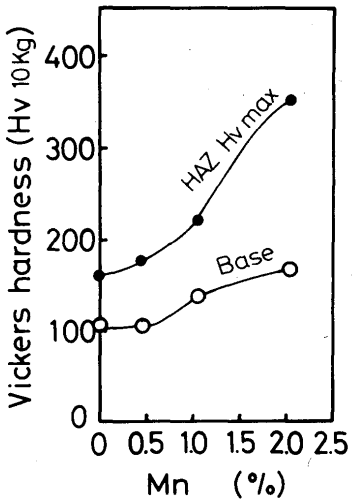


Fig. 8 Effect of Mn on the hardness in base metal and HAZ

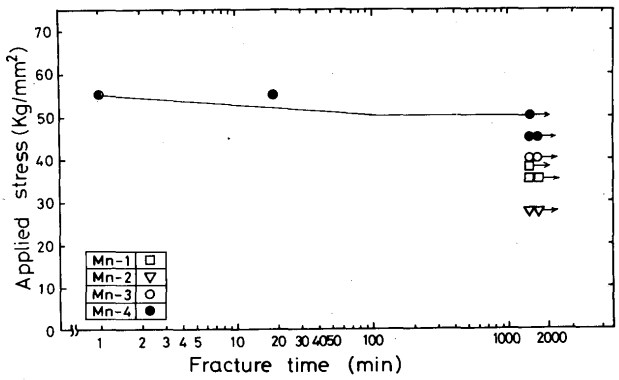


Fig. 9 Relation between applied stress and fracture time in Mn-alloyed steel

Mo-4 with an applied stress of 55 kg/mm$^2$ by SEM. Intergranular and quasi-cleavage fracture surfaces are seen in photo 9. The microstructure of the heat-affected zone in Mo-4 alloy steel is shown in **photo 10.** There is little ferrite along the prior-austenite grain boundary, and this well agreed with the result in CCT diagram by Inagaki et al[3].

### 3.4 Mn-alloyed steel

**Figure 8** shows the hardness of the base metal and the maximum hardness in the heat-affected zone. The maximum hardness shows a tendency to increase with manganese content. Delayed cracking was found only in Mn-4 steel whose maximum hardness showed about 350. **Figure 9** shows the relation between applied stress and fracture time. **Photograph 11** shows quasi-cleavage with hydrogen embrittlement in Mn-4 fractured in an applied stress of 55 kg/mm$^2$.

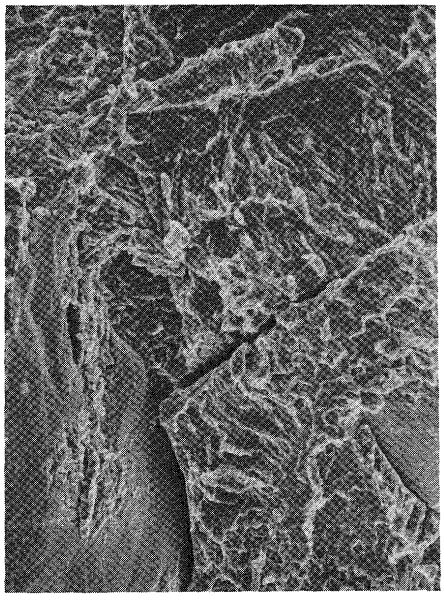

Photo 11. Example of microfractograph, Mn-4, $\sigma$=55 kg/mm$^2$, fracture time: 5.7 min, x 300

**Photograph 12** shows the microstructure of the heat-affected zone in Mn-3 and Mn-4 steels. There is little ferrite along the prior-austenite grain boundary in Mn-4, though a little ferrite is observed in Mn-3. It also well agreed with the CCT diagram by Inagaki et al[4].

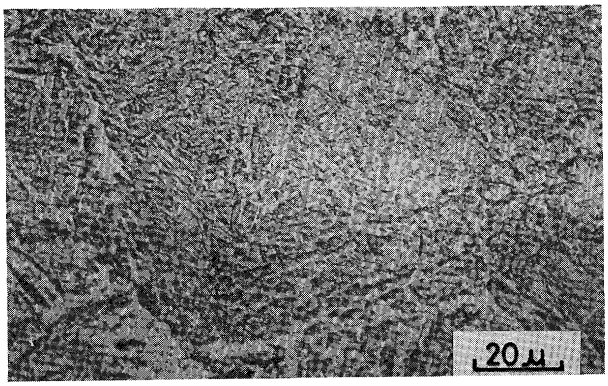


(a) Mn-3

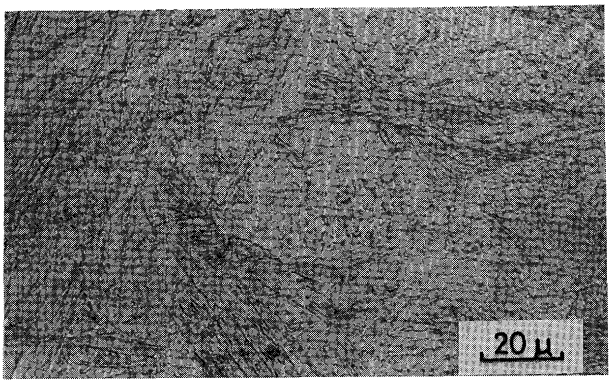


(b) Mn-4

**Photo 12.** Effect of Mn on microstructure in HAZ

## 4. Conclusion

(1) The delayed crack occurred in the 0.1%C basic steels in which contained alloying element more than about 5% in Ni, 4% in Cr, 1% in Mo or 2% in Mn.

(2) The maximum hardness in the heat-affected zone at which the delayed crack occurred was more than about 300 to 350 in Hv in the 0.1%C basic steels in which Ni, Cr, Mo and Mn are alloyed respectively.

(3) The microstructure of the heat-affected zone of the alloyed steels in which the delayed crack occurred mainly shows a bainitic and martensitic structure without proeutectoid ferrite along the prior-austenite boundary. In another word, it is roughly concluded from the knowledge within the range of this investigation that the delayed crack is difficult to occur in such steels in which the proeutectoid ferrite is well formed along the prior-austenite grain boundary in case of the cooling time of about 6 seconds from 800°C to 500°C. This feature was also suggested for commercial steels by the authors in the previous paper[5].

### Acknowledgement

We wish to thank Mr. T. Kasugai in the National Research Institute for Metals for furnishing the basic steels employed in this experiment.

### References

1) T. Kasugai and M. Inagaki: "Effects of Alloying Elements on Transformation Behaviour in Synthetic Weld Heat-affected Zone of Steels(V)," J. Japan Weld. Soc., Vol. 44(1975), pp. 687-692, (in Japanese).
2) T. Kasugai and M. Inagaki: "Effects of Alloying Elements on Transformation Behaviour in Synthetic Weld Heat-affected Zone of Steels (IV)," J.Japan Weld. Soc., Vol. 44(1975), pp. 323-331, (in Japanese).
3) T. Kasugai and M. Inagaki: "Effects of Alloying Elements on Transformation Behaviour in Synthetic Weld Heat-affected Zone of Steels (III)," J.Japan Weld. Soc., Vol. 44(1975), pp. 220-228, (in Japanese).
4) T. Kasugai and M. Inagaki: "Effect of Alloying Elements on Transformation Behaviour in Synthetic Weld Heat-affected Zone of Steels (I)," J.Japan Weld. Soc., Vol. 43(1974), pp. 1004-1012, (in Japanese).
5) F. Matsuda, H. Nakagawa, T. Tsuji and M. Tsukamoto "Effect of Hydrogen Content on Cold Crack Susceptibility of Various Steels with the Implant Test", Trans. of JWRI,. Vol. 7 (1978), No. 2, pp. 195-201.